DALTON
FULL PAPER

Influence of ligand backbones and counter ions on structures of helical silver(I) complexes with di-Schiff bases derived from phthalaldehydes and diamine

Hai-Liang Zhu, Ye-Xiang Tong and Xiao-Ming Chen *

School of Chemistry and Chemical Engineering, Zhongshan University, Guangzhou 510275, China. E-mail: cescxm@zsu.edu.cn

Received 29th June 2000, Accepted 14th September 2000
First published as an Advance Article on the web 27th October 2000

Five silver(I) complexes of Schiff bases, $[Ag_2L_2][ClO_4]_2$ **1**, $[Ag_2L_2][PF_6]_2 \cdot H_2O$ **2**, $[Ag_2L_2][NO_3]_2$ **3**, $^1_\infty[(AgL')(dnb)(H_2O)_{0.25}]$ (dnb = 3,5-dinitrobenzoate) **4** and $^1_\infty[(AgL')(NO_3)]$ **5** were synthesized, where L and L′ are derived from the [1 + 2] condensation of 2-(aminoethylamino)ethanol with isophthalaldehyde or terephthalaldehyde. Complexes **1**, **2**, **4** and **5** have been structurally characterised by X-ray crystallography, which shows that the cations in **1** and **2** have similar double helical structures, and **4** has a single-stranded helical structure. However, complex **5** exhibits a one-dimensional staircase-like structure. Each Ag atom in **1**, **2** and **4** adopts a highly distorted tetrahedral geometry, while that in **5** features a T-shaped geometry. In solution, **1**–**3** have virtually identical ^{1}H NMR spectra, similar FAB mass spectra and electrochemical properties.

Introduction

Double-helix formation of nucleic acids and self-assembly of viral protein coats are significant biologically.[1] Since the early pioneering work of Lehn on double-helical oligopyridyl copper(I) complexes,[2] there has been enormous interest in helical complexes. Self-assembly is a process by which organised supramolecular structures are spontaneously generated from their component molecular parts in high yield and specificity.[3] The approach involves the design of building blocks which contain metal-binding domains together with functionality required for the desired product. In recent years a very large number of self-assembled co-ordination polymers have been reported, of which many are silver(I) complexes.[3–8] Oligobipyridyl ligands have been designed to control the assembly of helicates. So far numerous helical complexes have been reported, including some of silver(I),[5–15] however only a few are double helicates.[9–15]

Metal helicates are generated when metals combine with ligands containing appropriate metallophilic and helical elements. Many different spacers, such as the ethylene group, have been used to link oligopyridyl or other multidentate entities.[16] The use of aromatic ligand backbones, such as 1,4- and 1,3-phenylene groups, as spacers for generation of single- and double-stranded transition metal helicates, respectively, is another approach previously suggested by Constable.[17]

We have recently reported a number of silver(I) complexes with different imidazole-containing di-Schiff bases, some of which exhibit helicity; the di-Schiff bases with aliphatic spacers usually form single-stranded helicates with silver(I) salts.[8] We expect that the 1,3-phenylene spacer is superior to aliphatic ones in the formation of double-stranded helical structures due to the lower rotational freedom imposed on the ligands. As a continuation of our studies on silver(I)–Schiff base complexes, we now report two new Schiff bases with 1,3-phenylene (L) or 1,4-phenylene spacers (L′) and the structures of their silver(I) complexes. Our results show that different counter ions do not control the assembly of the double-stranded helical silver(I) complexes containing L, however they can influence the assembly of silver(I) complexes with L′.

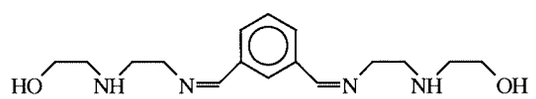

L

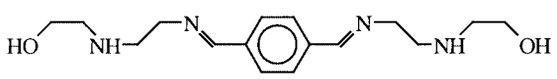

L′

Experimental

Materials and physical measurements

Reagents and solvents were used as commercially available. The C, H and N elemental analyses were carried out with a Perkin-Elmer 240Q elemental analyser. The cyclic voltammograms were measured on an electrochemical analyser over 2.0 to −2.0 V at room temperature, with a sample concentration of 1.0×10^{-4} mmol cm^{-3} in MeCN solution containing $Bu^n_4NPF_6$ (0.1 mmol cm^{-3}) and a scan speed of 100 mV s^{-1}. A platinum wire working electrode, platinum plate auxiliary electrode and saturated calomel electrode (SCE) reference electrode were employed. All potentials were measured with respect to the SCE and the experiments were carried out at *ca.* 20 °C. The FAB mass spectra were recorded on a VG ZAB-HS Autospectrophotometer, using 3-nitrobenzyl alcohol as matrix. The 500 MHz ^{1}H NMR spectra were measured in CD_3CN solution on an INOVA 500NB spectrometer with reference to internal $SiMe_4$.

CAUTION: although no problems were encountered in the preparation of the perchlorate salt, care should be taken when handing such a potentially explosive compound.

Preparations

L and L′. L (or L′) was prepared by the [1 + 2] condensation of terephthalaldehyde (or isophthalaldehyde) with 2-(amino-

 DOI: 10.1039/b005228k

ethylamino)ethanol in methanol at room temperature according to the literature procedure,[18] and further isolation was not carried out.

$[Ag_2L_2][ClO_4]_2$ 1. A solution of $AgNO_3$ (0.17 g, 1 mmol) in MeCN (5 cm^3) was added to a stirred MeOH (2 cm^3) solution containing 1 mmol of L. A few minutes later $NaClO_4$ (0.2 g) in MeOH (0.5 cm^3) was added dropwise. Slow diffusion of diethyl ether into the resulting solution for 24 h produced colourless crystals, which were collected by filtration, washed with MeCN and MeOH and dried in a vacuum desiccator over silica gel (yield 0.473 g, 92%). Calc. for $C_{16}H_{26}AgClN_4O_6$: C, 37.41; H, 5.10; N, 10.91%. Found: C, 37.01; H, 5.02; N, 11.10%.

$[Ag_2L_2][PF_6]_2 \cdot H_2O$ 2. A solution of $AgNO_3$ (0.17 g, 1 mmol) in MeCN (5 cm^3) was added to a stirred solution of L (1 mmol) in MeOH (2 cm^3). A few minutes later $NaPF_6$ (0.2 g) in MeOH (1.0 cm^3) was added dropwise. Treatment as above produced colourless crystals (yield 0.507 g, 90%). Calc. for $C_{34}H_{57}Ag_2F_{12}N_8O_5P_2$: C, 35.10; H, 4.94; N, 9.63%. Found: C, 34.88; H, 4.98; N, 9.55%.

$AgL(NO_3)$ 3. A solution of $AgNO_3$ (0.17 g, 1 mmol) in MeCN (5 cm^3) was added to a stirred solution of L (1 mmol) in MeOH (2 cm^3). Treatment as above produced colourless crystals. Owing to its good solubility in MeCN, complex **3** was only obtained in quite low yield (0.095 g, 10%). Calc. for $C_8H_{26}AgN_5O_5$: C, 25.27; H, 6.89; N, 18.42%. Found: C, 25.19; H, 7.01; N, 18.25%.

$^1_\infty[(AgL')(dnb)(H_2O)_{0.25}]$ 4. A solution of L′ (1 mmol) in MeOH (2 cm^3) was added to a stirred suspension of silver(I) 3,5-dinitrobenzoate Ag(dnb) (0.32 g, 1 mmol) in MeCN (5 cm^3) and Ag(dnb) immediately dissolved. Upon slow diffusion of diethyl ether into the resulting solution for 24 h, pale brown crystals were deposited. They were collected by filtration, washed with MeCN and MeOH and dried in a vacuum desiccator over silica gel. The yield was 163 g, 26%. Calc. for $C_{23}H_{29.5}AgN_6O_{8.25}$: C, 43.86; H, 4.72; N, 13.34%. Found: C, 43.55; H, 4.69; N, 13.26%.

$^1_\infty[(AgL')(NO_3)]$ 5. This was prepared by a similar procedure to that described for complex **3**, with L′ instead of L. The yield was 73%. Calc. for $C_8H_{13}AgN_3O_4$: C, 29.74; H, 4.06; N, 13.01%. Found: C, 30.00; H, 4.01; N, 12.93%.

^{1}H NMR spectra of complexes **1**, **2** and **3** are virtually identical within experimental errors: δ 2.66–2.68 (8 H, t), 2.90–2.92 (8 H, t, H_2CNCH_2), 3.54–3.56 (8 H, t, $=NCH_2$) and 3.72–3.74 (8 H, t, OCH_2). For **4**: δ 2.67–2.69 (8H, t), 2.90–2.92 (8H, t, H_2CNCH_2), 3.54–3.56 (8H, t, $=NCH_2$) and 3.74–3.76 (8H, t, OCH_2). Complex **5** has too weak ^{1}H NMR signals to be detected because of its insolubility in common organic solvents.

X-Ray crystallography

Diffraction intensities for complexes **1**, **2**, **4** and **5** were collected on a Siemens R3m diffractometer using Mo-Kα radiation ($\lambda = 0.71073$ Å). Lorentz-polarisation and absorption corrections were applied.[19] The structure solutions and full-matrix least-squares refinements based on F^2 were performed with the SHELXS 97[20] and SHELXL 97[21] program packages, respectively. All the non-hydrogen atoms were refined anisotropically. Hydrogen atoms of organic groups were generated geometrically and those of the aqua ligands located from the difference maps; all the hydrogen atoms were assigned isotropic thermal parameters and included in the structure-factor calculations. The two-fold disordered nitrate ions were refined with geometric restraints. Analytical expressions of neutral-atom scattering factors were employed, and anomalous dispersion corrections were incorporated.[22] The crystallographic data are summarised in Table 1. Selected bond distances and bond angles are given in Table 2.

CCDC reference number 186/2185.

See http://www.rsc.org/suppdata/dt/b0/b005228k/ for crystallographic files in .cif format.

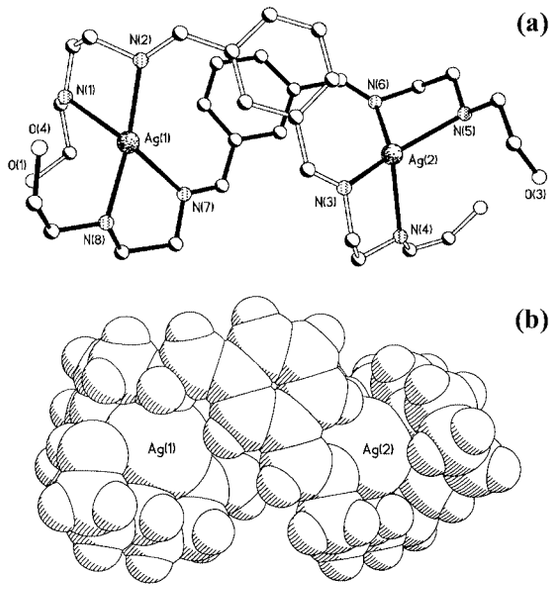

Fig. 1 Perspective (a) and space-filling (b) views of the helicate in complex **1**.

Results and discussion

Crystal structures of complexes 1 and 2

The crystal structures of $[Ag_2L_2][ClO_4]_2$ **1** and $[Ag_2L_2][PF_6]_2 \cdot H_2O$ **2** reveal that the complexes exist as discrete $[Ag_2L_2]^{2+}$ cations and counter anions in the solid. In the cation of **1** each ligand binds two Ag atoms in a bis-bidentate co-ordination mode, and forms the strand of the helix that twists around the helical axis on which the Ag atoms lie, as shown in Fig. 1. The pair of metal atoms are separated at 7.426(1) Å. Each Ag atom is tetrahedrally co-ordinated (Ag–N 2.298(6)–2.456(7) Å) by two bidentate chelate imine–amine entities from different L ligands, and the tetrahedron is severely distorted, as a result of the double chelate, with the intraligand N–Ag–N angles in the range 74.7(2) to 75.8(2)° and interligand N–Ag–N angles in the range 122.0(2) to 145.7(2)°. The average Ag–N distances (2.374 Å for **1** and 2.363 Å for **2**) are shorter than those (*ca.* 2.426 Å) found in oligobipyridyl silver(I) complexes.[13] The mean intraligand N–Ag–N angles (75.3° for both **1** and **2**) are comparable to those (75.8°) in the silver(I) complexes of ethylenediamine.[23] Although not shown, the double helicate in complex **2** has a very similar crystal structure to that in **1** with some minor geometric differences, as compared in Table 2. The metal–metal separation in complex **2** is 7.408(1) Å.

It is also noteworthy that π–π stacking interaction[24] between the pair of aromatic rings from two strands in the helicate plays an important role in stabilising the double-helical geometry, which is similar to those found for oligopyridyl silver(I) complexes. The pair of aromatic rings is aligned in a slightly off-set fashion, being approximately parallel to each other with dihedral angles of 18.1 and 10.4°, and the interplanar distances are 3.81 and 3.53 Å for complexes **1** and **2**, respectively.

Crystal structure of complex 4

Crystallography has established that complex **4** is composed of infinite one-dimensional chains, discrete carboxylates and lattice water molecules. There are two non-equivalent Ag atoms in the polymeric chain, each co-ordinated by two bridging L′

Table 1 Crystal data for complexes **1**, **2**, **4** and **5**

	1	**2**	**4**	**5**
Chemical formula	$C_{32}H_{52}Ag_2Cl_2N_8O_{12}$	$C_{34}H_{57}Ag_2F_{12}N_8O_5P_2$	$C_{23}H_{29.5}AgN_6O_{8.25}$	$C_8H_{13}AgN_3O_4$
M	1027.46	1127.50	629.90	323.08
Crystal symmetry	Monoclinic	Monoclinic	Triclinic	Monoclinic
Space group	$P2_1/c$	$C2/c$	$P\bar{1}$	$P2_1/n$
a/Å	15.651(4)	28.884(2)	12.429(2)	5.9580(10)
b/Å	14.455(4)	15.4220(1)	13.367(3)	13.909(4)
c/Å	20.466(4)	20.1870(10)	17.158(3)	14.576(7)
α/°			81.75(1)	
β/°	110.88(1)	90.310(4)	77.53(1)	90.75(2)
γ/°			78.70(1)	
V/Å^3	4326.1(18)	8992.1(10)	2714.1(9)	1207.8(7)
Z	4	8	8	4
T/K	293	293	293	293
μ(Mo-Kα)/mm^{-1}	1.093	1.038	0.800	1.672
No. measured data	6795	7262	9460	2108
No. observed data	3554	4977	4891	1261
$R1$ ($I > 2\sigma(I)$)	0.0664	0.0722	0.0690	0.0728
$wR2$ (all data)	0.1401	0.2249	0.1476	0.1270

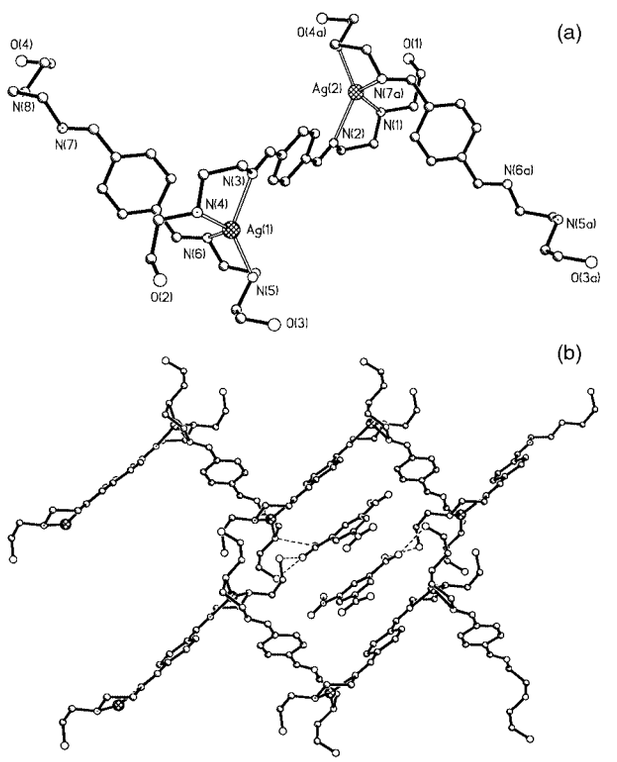

Fig. 2 Perspective views showing the co-ordination environments (a) and part of the two-dimensional layer (b) in complex **4**.

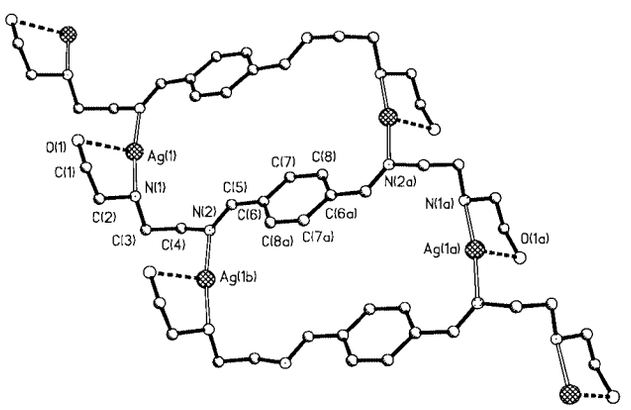

Fig. 3 Perspective view of the structural subunits of the staircase-like $^1_\infty$[AgL′] chain in complex **5**.

ligands through four nitrogen atoms (Ag–N 2.259(5)–2.444(5) Å) to form a severely distorted tetrahedral geometry, as illustrated in Fig. 2. The distortion of the co-ordination, with the intraligand N–Ag–N angles in the range 76.9(2)–77.4(2)° and interligand N–Ag–N angles in the range 114.2(2)–140.2(2)°, is also attributed to the bidentate chelate mode of the L′ ligands. The Ag–N bonds are comparable to those found in **1** and **2** and in other Schiff base-containing complexes.[8,25] On the other hand, all the bond distances between Ag atoms and imine nitrogen atoms are longer than those between Ag atoms and amine nitrogen atoms, which contrasts to the situation in other silver(I) complexes reported in this paper and in the literature.[25] The separation (9.758(2) Å) between adjacent Ag atoms in the helical chain of **4** is much longer than the intramolecular Ag···Ag distances in both **1** and **2**, which may be ascribed to the single-stranded structure in complex **4** as compared to the double-stranded structures in **1** and **2**, as well as to the geometric difference between the 1,3- and 1,4-phenylene spacers.

Finally, it should be mentioned that adjacent helical chains are arranged into two-dimensional networks containing rhombic cavities in the solid as shown in Fig. 2(b), in each of which two carboxylate anions are clathrated. The carboxylates are aligned in parallel with each other and with the 1,4-phenylene groups of the helical chains, featuring offset π–π stacking interactions with the interplanar distance between the two carboxylates and those between the carboxylate and the phenylene group being *ca*. 3.4 and 3.6 Å, respectively. Hydrogen bonds between the hydroxyl and carboxylate (or nitro) groups (O···O 2.67–2.77 Å) as well as those between the amine and carboxylate groups (N···O 2.86–2.94 Å) also play a role in consolidating the network structure.

Crystal structure of complex 5

The structure of complex **5** consists of polymeric cationic chains composed of $[AgL']^+$ units and unco-ordinated nitrate anions. As shown in Fig. 3, each Ag atom in the cationic chain is linearly co-ordinated by one amine and one imine nitrogen atom from different L′ ligands with the N–Ag–N angle of 172.5(3)°. It is notable that each amine/imine bidentate entity in the L′ ligand ligates two Ag atoms, different from the usual chelate mode found in complexes **1** and **2**. Such a bridging mode for a diimine-like bidentate entity is quite unusual, and has very recently been documented in our previous work.[8] Both Ag–N_{amine} (2.197(7) Å) and Ag–N_{imine} (2.159(6) Å) bond lengths are reasonable and comparable with those found in related complexes.[25] Each hydroxyl oxygen atom of the L′ ligand occupies the third co-ordination position of an Ag atom in the form of weak interaction (Ag–O 2.65(1) Å). Two Ag atoms and two L′ ligands constitute a 24-membered macrocycle with size

Table 2 Selected bond lengths (Å) and bond angles (°) for complexes **1**, **2**, **4** and **5**

1			
Ag(1)–N(2)	2.298(6)	Ag(1)–N(8)	2.313(5)
Ag(1)–N(7)	2.430(6)	Ag(1)–N(1)	2.456(7)
Ag(2)–N(3)	2.335(6)	Ag(2)–N(5)	2.366(6)
Ag(2)–N(6)	2.369(6)	Ag(2)–N(4)	2.391(6)
N(8)–Ag(1)–N(7)	74.7(2)	N(2)–Ag(1)–N(1)	75.5(2)
N(5)–Ag(2)–N(6)	75.7(2)	N(3)–Ag(2)–N(4)	75.8(2)
N(2)–Ag(1)–N(8)	145.7(2)	N(2)–Ag(1)–N(7)	128.5(2)
N(8)–Ag(1)–N(1)	116.4(2)	N(7)–Ag(1)–N(1)	122.0(2)
N(3)–Ag(2)–N(5)	140.7(2)	N(3)–Ag(2)–N(6)	132.4(2)
N(5)–Ag(2)–N(4)	112.5(2)	N(6)–Ag(2)–N(4)	125.7(2)
2			
Ag(1)–N(7)	2.353(7)	Ag(1)–N(3)	2.352(6)
Ag(1)–N(4)	2.356(6)	Ag(1)–N(8)	2.357(7)
Ag(2)–N(6)	2.235(6)	Ag(2)–N(1)	2.295(7)
Ag(2)–N(5)	2.443(6)	Ag(2)–N(2)	2.511(7)
N(3)–Ag(1)–N(4)	77.4(2)	N(7)–Ag(1)–N(8)	74.5(3)
N(1)–Ag(2)–N(2)	73.8(2)	N(6)–Ag(2)–N(5)	77.7(2)
N(7)–Ag(1)–N(3)	127.3(2)	N(7)–Ag(1)–N(4)	125.3(2)
N(3)–Ag(1)–N(8)	137.8(2)	N(4)–Ag(1)–N(8)	122.6(2)
N(6)–Ag(2)–N(1)	152.0(2)	N(6)–Ag(2)–N(2)	125.2(2)
N(1)–Ag(2)–N(5)	115.7(2)	N(5)–Ag(2)–N(2)	114.0(2)
4			
Ag(1)–N(5)	2.259(5)	Ag(1)–N(4)	2.304(4)
Ag(1)–N(3)	2.389(4)	Ag(1)–N(6)	2.632(6)
Ag(2)–N(8a)	2.258(4)	Ag(2)–N(1)	2.294(4)
Ag(2)–N(2)	2.444(5)	Ag(2)–N(7a)	2.644(6)
N(5)–Ag(1)–N(4)	139.6(2)	N(5)–Ag(1)–N(3)	135.3(2)
N(4)–Ag(1)–N(3)	77.4(2)	N(5)–Ag(1)–N(6)	70.8(2)
N(4)–Ag(1)–N(6)	123.4(2)	N(3)–Ag(1)–N(6)	114.2(2)
N(8a)–Ag(2)–N(1)	140.2(2)	N(8a)–Ag(2)–N(2)	133.7(2)
N(1)–Ag(2)–N(2)	76.9(2)	N(8a)–Ag(2)–N(7a)	70.6(2)
N(1)–Ag(2)–N(7a)	125.2(2)	N(2)–Ag(2)–N(7a)	115.2(2)
5			
Ag(1)–N(1)	2.197(7)	Ag(1)–N(2b)	2.159(6)
Ag(1)–O(1)	2.65(1)		
N(2b)–Ag(1)–N(1)	172.5(3)	N(2b)–Ag(1)–O(1)	108.1(3)
N(1)–Ag(1)–O(1)	74.9(3)		

Symmetry codes: for **4**, (a) $-x, -y, -z$; for **5**, (b) $-1 + x, y, z$.

ca. 5 × 10 Å, and the inter-linkage of the L′ ligand with Ag atoms results in infinite staircase-like chains, as illustrated in Fig. 3. All the phenylene rings in each chain are exactly parallel. The disordered nitrate anions form acceptor hydrogen bonds (O · · · N 2.84 Å) with the amine nitrogen atoms.

MS and ^{1}H NMR spectra

The FAB mass spectra provide evidence of the existence of $[Ag_2L_2]^{2+}$ double helicates of complexes **1**, **2** and **3**. The most abundant ions in 4-nitrobenzyl alcohol solution are the $[Ag_2L_2]^{2+}$ (m/z = 413, 415, relative abundance 100 and 82%), and the abundance of the "free" ligand L^+ (m/z = 307) is nearly 99%. The FAB mass spectrum of **4** displays similar patterns to those of the former complexes, and has peaks at m/z 413, 415 and 307 (relative abundances 97, 80 and 100%) due to $[AgL']^+$ and L'^+, respectively, in accord with the crystal structures.

The identical ^{1}H NMR spectra of complexes **1**, **2** and **3** in DMSO-d_6 solution indicate very similar structures in solution, although the crystal structures are slightly different in detail. The signals of aliphatic protons occur in the region δ 2.66–3.74. The signals of the aromatic protons are well resolved, in the region δ 7.37–8.52. The splittings of the signals of the aromatic protons of **1**–**3** at *ca.* δ 7.64 may be attributed to the intramolecular π–π stacking interaction.[14,26] The ^{1}H NMR spectrum of complex **4** in DMSO-d_6 solution is very similar to those of **1**–**3** in the aliphatic region δ 2.67–3.76. However, the signals of the aromatic protons (δ 7.65–7.67) are complicated and are significantly different from those of **1**–**3**.

Table 3 CV data for complexes **1**, **2**, **3** in MeCN at room temperature

Complex	E_{pc1}/V	E_{pc2}/V	E_{pc3}/V	E_{pa1}/V	E_{pa2}/V
1	−0.08	−0.24	−1.10	+0.35	+1.15
2	−0.08	−0.26	−1.13	+0.34	+1.15
3	−0.08	−0.24	−1.14	+0.35	+1.17

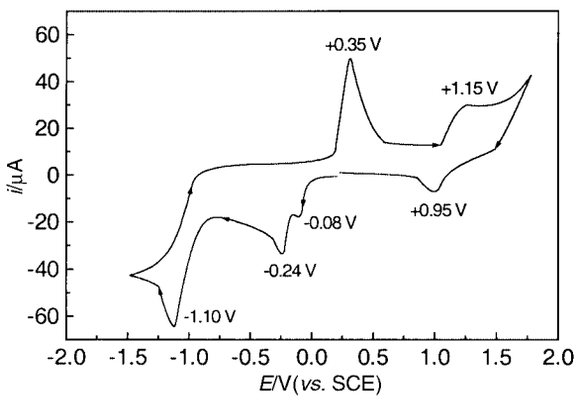

Fig. 4 Cyclic voltammogram of complex **1** in MeCN at room temperature with 0.1 mmol cm^{-3} of Et_4NClO_4 as electrolyte at a platinum electrode with a SCE as reference. Conditions: 1.0×10^{-4} mol L^{-1}, v = 100 mV s^{-1}.

Electrochemistry

Complexes **1**, **2** and **3** underwent overall cyclic voltammetry (CV) processes in CH_3CN containing Et_4NClO_4 (0.1 mmol cm^{-3}) in the range 2.0 to −2.0 V at room temperature starting with reduction, and the data are summarised in Table 3. The electrochemical behaviours of **2** and **3** are quite similar to that of **1**, which is shown in Fig. 4. The cathodic waves occur with reduction peaks at about −0.08 and −0.24 V, which indicate the formation of two valence states $[Ag^IAg^0L_2]^+$ and $[Ag^0Ag^0L_2]$ respectively. The number of electrons consumed at each step was confirmed to be one as the peak current ratio of the cathodic waves was about 1:1. The irreversible cathodic wave is at about −1.10 V and gas was evolved upon reduction due to decomposition of the complexes and then $2L + 4e \longrightarrow 2L^- + 2H_2$.[25] The anodic wave at about +0.35 V has been confirmed by comparing it with the standard oxidation potential of Ag–Ag$^+$ in MeCN (+0.23 V *vs.* SCE). The potential shift of 0.12 V indicates that co-ordination of the N_4O_2 donor set significantly stabilises the Ag^0 in these complexes. Since the peak current ratio of the cathodic wave at −0.08 V and the anodic wave at +0.35 V was about 1:2, the anodic wave is probably caused by the one-step oxidation reaction $[Ag^0Ag^0L_2] - 2e \longrightarrow [Ag^IAg^IL_2]^{2+}$. The pseudo-reversible redox couple at +1.15/+0.95 V (see Fig. 4) has been confirmed to be $[Ag^{II}Ag^{II}L_2]^{4+} + 2e \longrightarrow [Ag^IAg^IL_2]^{2+}$ by comparing it with the standard oxidation potential of Ag^+–Ag^{2+}. The electrochemical process may be expressed as in Scheme 1. These observations suggest that the ligand can stabilise the silver(I) ions in the complexes.

Discussion

Based on the literature and our previous work,[6,8] we designed two new, readily prepared di-Schiff base ligands, L and L′. The structure of L enables it to form double-stranded silver(I) helicates easily, independent of the counter ions, in contrast to the fact that silver(I) complexes and co-ordination polymers are

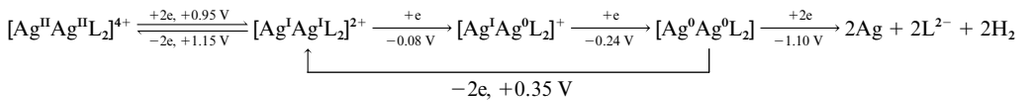

Scheme 1

easily influenced by the counter ions.[4,6,25] On the other hand, with a 1,4- instead of a 1,3-phenylene group, L′ behaves markedly differently in the assembly process, generating silver(I) complexes with different structures dependent on the counter ions and the π–π stacking interaction. Based on current results, we may suggest that the helicity of silver(I) complexes may be controlled by the phenylene spacer of the ligand, and a 1,3-phenylene spacer is superior in the formation of double-stranded helical structures. Finally, the two hydroxyl groups in L, which are first introduced into the ends of a dinucleating helical strand, greatly increase the solubility of the double helicates in various polar solvents including water.

Acknowledgements

We acknowledge financial support by the National Natural Science Foundation of China (No. 29971033 and 29625102). We thank the Chemistry Department of the Chinese University of Hong Kong for donation of the diffractometer.

References

1 A. Klug, *Angew. Chem.*, *Int. Ed. Engl.*, 1983, **22**, 565.
2 J.-M. Lehn, *Angew. Chem.*, *Int. Ed. Engl.*, 1988, **27**, 89; T. M. Garrett, U. Koert, J.-M. Lehn, A. Rigault, D. Meyer and J. Fischer, *J. Chem. Soc.*, *Chem. Commun.*, 1990, 557.
3 L. Carlucci, G. Ciani, D. M. Proserpio and A. Sironi, *J. Am. Chem. Soc.*, 1995, **117**, 4562; L. Carlucci, G. Ciani, D. W. V. Gudenberg, D. M. Proserpio and A. Sironi, *Chem. Commun.*, 1997, 631; K. A. Hirsch, S. R. Wilson and J. S. Moore, *Chem. Commun.*, 1998, 13; K. A. Hirsch, S. R. Wilson and J. S. Moore, *Chem. Eur. J.*, 1997, **3**, 765; A. J. Blake, N. R. Champness, A. Khlobystov, D. A. Lemenovskii, W.-S. Li and M. Schröder, *Chem. Commun.*, 1997, 2027; J. A. R. Navarro, J. M. Salas, M. A. Romero and R. Faure, *J. Chem. Soc.*, *Dalton Trans.*, 1998, 901; C. B. Aakeröy and A. M. Beatty, *Chem. Commun.*, 1998, 1067; C. Janiak, T. G. Scharman, P. Albrecht, F. Marlow and R. Macdonald, *J. Am. Chem. Soc.*, 1996, **118**, 6307; M.-L. Tong, X.-M. Chen, B.-H. Ye and L.-N. Ji, *Angew. Chem.*, *Int. Ed.*, 1999, **38**, 2237; M.-L. Tong, S.-L. Zheng and X.-M. Chen, *Chem. Commun.*, 1999, 561.
4 H.-P. Wu, C. Janiak, G. Rheinwald and H. Liang, *J. Chem. Soc.*, *Dalton Trans.*, 1999, 183; C. Janiak, L. Uchlin, H.-P. Wu, P. Klufers, H. Piotrowski and T. G. Scharman, *J. Chem. Soc.*, *Dalton Trans.*, 1999, 3121; M.-L. Tong, S.-L. Zheng and X.-M. Chen, *Chem. Eur. J.*, 2000, **6**, 3729.
5 M. Munakata, L. P. Wu and T. Kuroda-Sowa, *Adv. Inorg. Chem.*, 1999, **46**, 173 and references therein.
6 M.-L. Tong, X.-M. Chen, B.-H. Ye and S. W. Ng, *Inorg. Chem.*, 1998, **37**, 5278; G. Yang, S.-L. Zheng and X.-M. Chen, *Inorg. Chim. Acta*, 2000, **233**, 86.
7 P. K. Bowyer, K. A. Porter, A. D. Rae, A. C. Willis and S. B. Wild, *Chem. Commun.*, 1998, 1153.
8 S.-P. Yang, X.-M. Chen and L.-N. Ji, *J. Chem. Soc.*, *Dalton Trans.*, 2000, 2337; S.-P. Yang, H.-L. Zhu, X.-H. Yin, X.-M. Chen and L.-N. Ji, *Polyhedron*, 2000, **19**, in press.
9 E. C. Constable, S. M. Elder, M. J. Hannon, A. Martin, P. R. Raithby and D. A. Tocher, *J. Chem. Soc.*, *Dalton Trans.*, 1996, 2423.
10 E. C. Constable, M. J. Hannon, A. Martin, P. R. Raithby and D. A. Tocher, *Polyhedron*, 1992, **11**, 2967.
11 E. C. Constable, J. M. Holmes and P. R. Raithby, *Polyhedron*, 1991, **10**, 127.
12 E. C. Constable, A. J. Edwards, P. R. Raithby and J. V. Walker, *Angew. Chem.*, *Int. Ed. Engl.*, 1993, **32**, 1465.
13 Y. Fu, J. Sun, Q. Li, Y. Chen, W. Dai, D. Wang, T. C. W. Mak, W. Tang and H. Hu, *J. Chem. Soc.*, *Dalton Trans.*, 1996, 2309.
14 P. K.-K. Ho, S. M. Peng, K.-Y. Wong and C.-M. Che, *J. Chem. Soc.*, *Dalton Trans.*, 1996, 1829.
15 M. J. Hannon, C. L. Painting and N. W. Alcock, *Chem. Commun.*, 1999, 2023.
16 V. Balzani, *Tetrahedron*, 1992, **48**, 10443.
17 E. C. Constable, *Tetrahedron*, 1992, **48**, 10013.
18 R. Menif and A. E. Martell, *J. Chem. Soc.*, *Chem. Commun.*, 1989, 1521; D. Chen and A. E. Martell, *Tetrahedron*, 1991, **47**, 6895.
19 A. C. T. North, D. C. Phillips and F. S. Mathews, *Acta Crystallogr.*, *Sect. A*, 1968, **24**, 351.
20 G. M. Sheldrick, SHELXS 97, Program for Crystal Structure Determination, University of Göttingen, 1997.
21 G. M. Sheldrick, SHELXL 97, Program for Crystal Structure Refinement, University of Göttingen, 1997.
22 *International Tables for Crystallography*, Kluwer Academic Publishers, Dordrecht, 1992, vol. C, Tables 4.2.6.8 and 6.1.1.4.
23 E. Bang, *Acta Chem. Scand.*, *Ser. A*, 1978, **32**, 555.
24 C. A. Hunter and J. K. Sanders, *J. Am. Chem. Soc.*, 1990, **112**, 5525; C. Janiak, *J. Chem. Soc.*, *Dalton Trans.*, 2000, 3885.
25 H.-L. Zhu, Y.-X. Tong, L.-S. Long, M.-L. Tong and X.-M. Chen, *Supramol. Chem.*, 1999, **11**, 119.
26 M.-L. Tong, B.-H. Ye, J.-W. Cai, X.-M. Chen and S. W. Ng, *Inorg. Chem.*, 1998, **37**, 2645.